

AD-A089 071

LASER ANALYTICS INC BEDFORD MA

F/G 7/4

HIGH RESOLUTION TUNABLE DIODE LASER MEASUREMENTS OF WATER VAPOR--ETC(U)

OCT 79 R S ENG, A W MANTZ, C G VENKATESH

F19628-77-C-0015

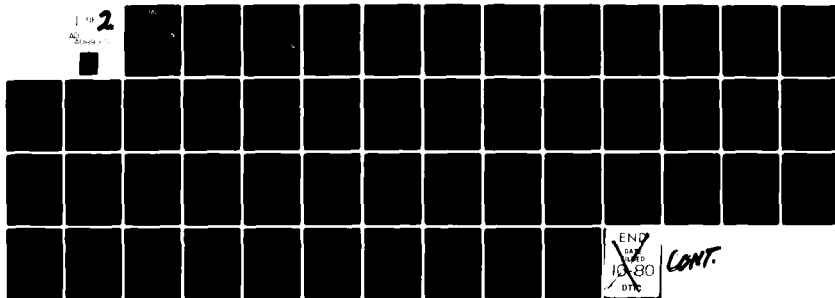
UNCLASSIFIED

AFGL-TR-79-0239

NL

2

AD-A089 071



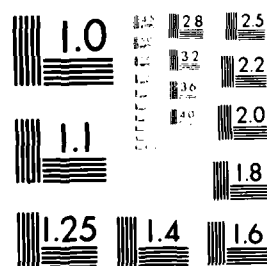
END
X
10-80
DTIC

CONT.

1 OF 2

AD.

A089071



MICROCOPY RESOLUTION TEST CHART
NATIONAL BUREAU OF STANDARDS - 1963-A

SL

LEVEL

(12)

AFGL-TR-79-0239

**HIGH RESOLUTION TUNABLE DIODE LASER MEASUREMENTS
OF WATER VAPOR CONTINUUM ABSORPTION AND
THEORETICAL FEASIBILITY STUDY OF WATER
VAPOR LINESHAPED BY DOUBLE RESONANCE
SPECTROSCOPY**

R.S. Eng
A.W. Mantz
C.G. Venkatesh

Laser Analytics, Inc.
25 Wiggins Avenue
Bedford, MA 01731

Final Report
March 1978 - 30 September 1979

15 October 1979

Approved for public release; distribution unlimited

AIR FORCE GEOPHYSICS LABORATORY
AIR FORCE SYSTEMS COMMAND
UNITED STATES AIR FORCE
HANSCOM AFB, MASSACHUSETTS 01731

DTIC
ELECTE
SEP 11 1980
S C D

80 9 11 003

AD A089071

DDC FILE COPY

Qualified requestors may obtain additional copies from the Defense Documentation Center. All others should apply to the National Technical Information Service.

Unclassified

SECURITY CLASSIFICATION OF THIS PAGE (When Data Entered)

REPORT DOCUMENTATION PAGE		READ INSTRUCTIONS BEFORE COMPLETING FORM
1. REPORT NUMBER (18) AFGL-TR-79-0239	2. GOVT ACCESSION NO. AD-A089 07	3. RECIPIENT'S CATALOG NUMBER (19)
4. TITLE (and Subtitle) High Resolution Tunable Diode Laser measurements of water vapor continuum absorption and theoretical feasibility study of water vapor lineshape by double resonance spectroscopy.		5. TYPE OF REPORT & PERIOD COVERED Final Report, Mar 1978-30 Sep 79, September 30, 1979
7. AUTHOR(S) (10) R. S. / Eng, A. W. / Mantz and C. G. / Venkatesh		6. PERFORMING ORG. REPORT NUMBER FINAL REPORT
9. PERFORMING ORGANIZATION NAME AND ADDRESS Laser Analytics, Inc. 25 Wiggins Avenue Bedford, MA 01730		8. CONTRACT OR GRANT NUMBER(s) (15) F19628-77-C-0015
11. CONTROLLING OFFICE NAME AND ADDRESS Air Force Geophysics Laboratory Hanscom AFB MA 01731 Monitor/Shepard A. Clough/OPI		10. PROGRAM ELEMENT, PROJECT, TASK AREA & WORK UNIT NUMBERS 61102F (16) 2310GLAD (17) G 1
14. MONITORING AGENCY NAME & ADDRESS (if different from Controlling Office) (11) 15 Oct 77 (12) 50		12. REPORT DATE October 15, 1979
		13. NUMBER OF PAGES 51
		15. SECURITY CLASS. (of this report) Unclassified
		15a. DECLASSIFICATION/DOWNGRADING SCHEDULE
15. DISTRIBUTION STATEMENT (of this Report) Approved for public release; distribution unlimited.		
17. DISTRIBUTION STATEMENT (of the abstract entered in Block 20, if different from Report)		
18. SUPPLEMENTARY NOTES		
19. KEY WORDS (Continue on reverse side if necessary and identify by block number) High-Resolution Infrared Absorption Spectra of H ₂ O and CO ₂ , linewidth, line intensity, lineshape, continuum absorption Tunable Diode Laser Spectroscopy.		
20. ABSTRACT (Continue on reverse side if necessary and identify by block number) Water vapor continuum absorption was measured in the 900-1050 cm ⁻¹ region using tunable diode laser and a 1-M base White cell at 296 K and 337 K. Both continuous and spot frequency absorption show pressure squared dependence. The high resolution technique takes into account local line absorption very well in determining the continuum absorption. Results show a slightly weaker temperature dependence for the continuum absorption.		

DD FORM 1473

EDITION OF 1 NOV 65 IS OBSOLETE

Unclassified

SECURITY CLASSIFICATION OF THIS PAGE (When Data Entered)

411 836

DTIC
ELECTE
SEP 11 1980
S C D

20

A proposed double resonance spectroscopic technique is described in which a CO laser in coincidence with a water vapor line is used to pump the water vapor transition and a CW Tunable Diode Laser is used to probe the water vapor absorption coefficient up to 100 halfwidths from the pressure broadened line to determine the lineshape.

TABLE OF CONTENTS

1.0	INTRODUCTION	Page 1
2.0	SUMMARY OF PROGRESS IN PHASE I AND PHASE II	Page 1
3.0	SUMMARY OF PROGRESS IN THE FINAL PHASE OF THE PROGRAM	Page 3
4.0	PREPRINT	Page 8
5.0	DOUBLE RESONANCE SPECTROSCOPY FEASIBILITY REPORT	Page 26

Accession For	
NTIS GRA&I	<input checked="checked" type="checkbox"/>
DDC TAB	<input type="checkbox"/>
Unannounced	<input type="checkbox"/>
Justification	
By _____	
Distribution/	
Availability Codes	
Dist	Avail and/or special
<i>R</i>	

1.0 INTRODUCTION

This is a final report for the study program, the major goal of which is to perform high resolution tunable diode laser absorption measurements of water vapor in the $950\text{--}1050\text{ cm}^{-1}$ atmospheric window with emphasis on understanding of the continuum absorption. As originally outlined, the program is to have three phases covering three fiscal years from December 1, 1976 through September 30, 1979.

2.0 SUMMARY OF PROGRESS IN PHASE I AND PHASE II

In the first phase, which is the first fiscal year, the objectives are to purchase the major equipment items and to assemble and integrate them into a diode laser spectrometer system. A heatable multiple-pass cell with adjustable pathlength up to 4050 cm was purchased and integrated into the laser spectrometer system. Other equipment of significant importance were a capacitance manometer with a 1% full-scale accuracy and a dew-point hygrometer for water vapor partial-pressure measurements. The cell was heated to about 110°C by insulated heating tapes and the temperature was controlled to about $\pm 2^{\circ}\text{C}$ using a controller.

Early in the experimental phase, a variation in beam transmittance as much as 10% was noted when the cell pressure was changed from vacuum to atmospheric. We attributed this to a slight deflection of the objective mirrors inside the cell. Therefore, the background absorption measurements were always

obtained with the cell filled with nitrogen at the same pressure used in the sample scan. Digital recording was incorporated near the end of the first fiscal year. The measurements used a single-beam setup. A frequency scale was generated by recording the transmission peaks of a 2.5906 cm^{-1} Ge etalon. The line positions are from the AFGL Line Parameter Listing.

The absorption line parameters including self- and nitrogen-broadening coefficients of 17 H_2O lines in the 10 to 15 μm spectral region have been measured. Many of the H_2O lines are pure rotational lines, and their linewidths exhibit the expected general narrowing trend as the rotational quantum number increases. The details of the experiment and measurement results have been reported in a published journal article⁽¹⁾.

In the second phase of the program, we studied the lineshape of carbon dioxide gas instead of water vapor, because it was felt that it was a simpler molecule for an initial study of continuum absorption. In particular, we selected the Q-branch head of the $10^0_0 + 01^1_0$ band near 618 cm^{-1} for study. The Q-branch lines are closely spaced so that the wings of many of the Q-branch lines contribute significantly to the absorption continuum near the branch head (between Q(2) and R(1)). The intensity and linewidths of about 12 Q-branch lines were measured at different total pressures for both pure CO_2 and $\text{N}_2:\text{CO}_2$ mixtures to determine the broadening coefficients.

Because the Q-branch lines are so close together (except for high J lines), it was rather difficult to determine the background level accurately even at 100 Torr of pressure. For this reason, it was decided to measure the comparatively well-separated CO₂ lines in other bands--namely, the 01¹0 + 00⁰0, 00⁰1 + (00⁰1, 02⁰0) I and the 00⁰1 + (00⁰1, 02⁰0) II bands--assuming that the linewidth varies very little from band to band. All together about 11 ν_2 band lines were measured.

Two lines in the well-known laser emission bands at 10.4 μm and 9.4 μm were measured at both room temperature and at about 383 K for the determination of the temperature dependence of linewidth. The details of the experiment and measurement results have been reported in a published journal article.⁽²⁾

3.0 SUMMARY OF PROGRESS IN THE FINAL PHASE OF THE PROGRAM

In the final phase (third year of the program, two projects were undertaken in connection with the water vapor continuum absorption measurements. The first project was the investigation into the feasibility of studying the far-wing (50 - 100 Lorentzian halfwidths from a line center) absorption of water vapor lines. The motivation behind this investigation is that the continuum absorption is caused by the sum of the far-wing absorptions of many strong water vapor lines. By knowing the lineshape, one hopes to be able to predict the continuum absorption throughout the mid-infrared spectral region.

Briefly, we disturb the population distribution by pumping at or near the line center of a strong water vapor line with a pulsed laser of moderate peak power and probe the absorption coefficient with a CW tunable diode laser at appropriate spectral distances (up to 100 Lorentzian halfwidths) from the line center.

Calculations show that for the moderately strong water vapor line at 1923.16 cm^{-1} , with 100 Torr (total) water vapor pressure, and a 100 cm pathlength, the absorbance, αL , is about 0.0013 at 100 halfwidths from line center. The percentage change in αL due to the pump (a pulsed CO laser) is about 3.7 percent for a pump power density of 1 kW-cm^{-2} and a relaxation time " t_2 " of 10 ns. In absolute term, the change in absorbance is then 4.81×10^{-5} , which is well above the value of 1×10^{-6} ordinarily detectable in Stark spectroscopy with which the present proposed experimental technique has a lot in common.

The experiment would use a small multipass cell to increase the pathlength and pump power density and a Q-switched CO laser which has a transition in near coincidence with the water vapor absorption. The results of the theoretical calculations and proposed experimental investigation for water vapor lineshape study has been reported in quarterly reports and is included here.

Due to the high cost of the additional equipment required, we did not perform the experiment, instead we pursued the measure-

ment for continuum absorption using tunable diode lasers. The next paragraph summarizes the efforts and results on this subject.

On account of the fact that the 40 m commercial cell used in the earlier parts of the program had background instability problems associated with changes in cell pressure, a Laser Analytics designed 1 m base multipass cell with superior mechanical features was used for the continuum absorption measurements. Using this cell, the transmittance instability associated with cell pressure change mentioned for the 40 m cell was completely absent for a pressure change from vacuum to one atmosphere. Additionally larger pathlengths (80 m to 100 m) were employed, and the temperature was varied from room to about 64°C.

High resolution scans in the $900\text{--}1050\text{ cm}^{-1}$ spectral region show that the continuum absorption coefficient is proportional to the pressure squared and exponentially to the negative of the absolute temperature. Both continuous and spot frequency absorptions were measured. In the vicinity of strong water vapor lines, the observed profile shows a Lorentzian shape and a smooth continuum. The continuum absorption vs frequency at room temperature is in close agreement with that reported by Burch et al;⁽¹⁾ at higher temperatures our observed absorption coefficient is slightly higher, implying a weaker temperature dependence than that reported by Selby et. al. in the AFGL LOWTRAN 3B,⁽²⁾ which summarizes previous continuum absorption works including Ref. 1.

The results have been presented at the Water Vapor Workshop at Vail, Colorado, September 11-13, 1979, and the paper will be published in the Proceeding of the Water Vapor Workshop in the near future. The paper in its preprint form is included here as a scientific report.

REFERENCES

1. R. S. Eng and A. W. Mantz, J. Mol. Spectrosc. 74, 388 (1979).
2. R. S. Eng and A. W. Mantz, J. Mol. Spectrosc. 74, 331 (1979).
3. D. E. Burch, "Investigation of the Absorption of Infrared Radiation by Atmospheric Gases," Semiannual Technical Report, Aeronutronic Division, Philco Ford Corporation, Aeronutronic Report U-4784 (30 January 1971).
4. J. E. A. Selby, E. P. Shettle, and R. A. McClatchey, "Atmospheric Transmittance from 0.25 to 28.5 μ m: Supplement LOWTRAN 3B (1976)" AFGL-TR-0258 ERP 587 (7 November 1976).
5. R. S. Eng and A. W. Mantz, "Tunable Diode Laser Measurements of Water Vapor Continuum and Water Vapor Absorption Lineshape in the 10 μ m Atmospheric Window Region", a paper presented at the Workshop on Atmospheric Water Vapor, organized by the Institute for Atmospheric Optics and Remote Sensing, Vail, Colorado (11-13 September 1979).

4.0

TUNABLE DIODE LASER MEASUREMENTS
OF WATER VAPOR CONTINUUM AND WATER VAPOR ABSORPTION LINE SHAPE
IN THE 10 μm ATMOSPHERIC TRANSMISSION WINDOW REGION*

R. S. Eng and A. W. Mantz

Laser Analytics, Inc.
25 Wiggins Avenue
Bedford, MA 01730

ABSTRACT

Water vapor line and continuum absorption in the 900 to 1050 cm^{-1} region was measured with a diode laser spectrometer and a heatable 100m White cell. High resolution scans show that the continuum absorption coefficient is proportional to the pressure squared and exponentially to the negative of the absolute temperature. In the vicinity of strong water vapor lines, the observed profile shows a Lorentzian shape and a smooth continuum.

*This research was supported by the Air Force Geophysics Laboratory, Bedford, MA under Contract No. F19628-77-C-0015; monitor: Dr. S. A. Clough.

INTRODUCTION

In the very important $10\mu\text{m}$ atmospheric window region, water vapor line and continuum absorptions are the dominant factors determining the overall transmittance over long atmospheric paths. There have been numerous laboratory spectroscopic measurements performed in recent years in the $10\mu\text{m}$ and other spectral regions using grating instruments and multiple-pass cells.⁽¹⁻⁵⁾ With the advent of CO_2 , CO , HF , and DF high power lasers, H_2O vapor continuum absorption measurements were performed at numerous emission lines of these fixed frequency lasers using both long path absorption cells⁽⁶⁻⁸⁾ and spectrophones.⁽⁸⁻¹⁰⁾ All of these measurements had showed that the water vapor continuum absorption coefficient was proportional to the square of the water vapor pressure and exponentially to the negative of the absolute temperature.

Along with these measurement efforts came the inevitable question: Is the water vapor continuum absorption due to local water vapor dimer absorption bands⁽¹¹⁾ or the sum of all absorptions at the far wings of strong H_2O lines having lineshape of the Van Vleck-Weisskopf type?^(12,13) Absorption by dimer as the continuum absorption source was first suggested by Varanasi⁽²⁾ and detailed approaches for spectral investigation were suggested by Braun and Leidecker.⁽¹⁴⁾ However, absorption at the far wings of lines has also been shown to have exactly the same pressure and similar temperature dependences.⁽¹⁵⁾

It appeared that a systematic approach to find answers to that question was in order. Leading the way, the Air Force Geophysics Laboratory has sponsored a number of research projects aiming towards a better understanding of the H_2O continuum absorption characteristics. In particular, Burch et. al.⁽¹⁶⁾ extended their continuum absorption to the $330\text{--}825\text{ cm}^{-1}$ region to obtain a frequency dependence over a wider range. Using tunable diode lasers Eng and Mantz⁽¹⁷⁾ performed accurate high-resolution H_2O linewidth and intensity measurements in the $10\mu\text{m}$

region to ascertain that absorption by local lines is better accounted for. Davies and Oli (18) performed theoretical investigation of H_2O linewidth and pressure shift to obtain better molecular interaction models. Recent rapid improvement in the resolution of the Fourier transform spectrometer has also aided the accurate determination of the water vapor line positions,^(19,20) which are needed in the calculations of absorption by local lines which have been found to be Lorentzian in the neighborhood of the line center.⁽²¹⁾ Having measured many H_2O lines in the $10\mu m$ region, (17) we pursued the present work in a continued effort in the understanding of the H_2O continuum absorption by performing measurements on the continuum absorption coefficient itself. To our knowledge, Montgomery was the only other investigator who used diode laser to measure H_2O vapor continuum absorption. He limited his measurements to region between H_2O lines and at essentially one narrow frequency region near 1250 cm^{-1} . Roberts et. al. (23) have summarized and evaluated the work of Burch and others on H_2O continuum absorption (see references cited in Ref. 23) and Selby et. al. (24) have used the results from Ref. 23 for atmospheric transmission calculations. These last two references contain simple empirical formulae for calculating the H_2O continuum absorption.

EXPERIMENTAL DETAILS

To measure the water vapor lineshape and continuum absorption, we used a laser spectrometer (Laser Analytics Inc. Model LS-3) and a 1-m base multiple pass cell (Laser Analytics Inc. Model LO-3) adjusted to have a total path length about 80m. Figure 1 is a schematic diagram of the experimental setup. The PbSnSe diode laser is mounted on a vibrationally isolated cold finger of a closed-cycle cooler. The temperature of the cold finger is stabilized to about 0.0003K throughout the range 10K to over 100K. The laser beam is collimated by an $f/1$, 2.54cm focal length lens and is focussed by an $f/2$, 5.08cm focal length lens on the entrance slit of a 0.5m grating monochromator (part of the Model LS-3 Spectrometer). A 400Hz chopper is used to

modulate the laser beam before the entrance slit. At the exit slit, the beam is directed into the multiple pass cell through a set of transfer optics consisting of an f/8, 20.32cm focal length concave spherical mirror and an f/11, 27.94cm focal length concave spherical mirror. The output beam from the cell is recollimated and goes through a 2.54cm Ge etalon for relative frequency calibration and is finally focussed on a HgCdTe detector with a 1mm x 1mm detector element. The output of the detector is pre-amplified and then synchronously detected with a lock-in amplifier. An 11-bit A/D converter digitizes the lock-in amplifier output signal for storage. The multiple pass cell is of the White type with an f/20 optics. The field mirror has a width of 57.15mm, allowing a reasonably wide image separation for 80 to 100m path-length operation. The cell body is made of stainless steel; both exhaust and gas filling ports are located at the center of the cell body to minimize contamination of the mirrors. Distilled water was used for filling. It was found necessary to neutralize the minute amount of NH_4OH present in distilled or deionized water with a drop of HCl to prevent non-negligible interference from strong ammonia vapor lines in the $10\mu\text{m}$ spectral region. Pressure is read to 1% accuracy with an MKS Model 221A capacitance manometer with a full scale of 100 torrs. A digital thermometer, Fluke Model 2100A, is used to monitor the cell body temperature at five places along the cell wall which was heated by heating tapes and insulated thermally from the room air convection. Water vapor was let into the cell slowly by evaporation from a water reservoir about 2.54cm in diameter. The reservoir was heated slightly to increase the saturation vapor pressure.

After a few trials, it was found that the most reproducible results were obtained by adhering to the following measurement procedure:

- (1) Fill the cell slowly to the desired pressure, usually less than 80% of the saturation vapor pressure.
- (2) Let the cell pressure stabilize for about 5 to 10 minutes.

- (3) The signal at the detector is then maximized by adjusting the micrometer screws holding the detector focusing lens and the pathlength adjusting screw in the multiple pass cell.
- (4) A sample scan is performed by digitally driving the diode laser current and the output voltage of the lock-in amplifier is sampled and stored.
- (5) The cell is quickly evacuated after the sample scan.
- (6) A reference or background scan is then performed and the lock-in amplifier voltage is sampled and stored.

In the sample and reference scans, the diode laser current is driven exactly over the same range to produce essentially identical laser output characteristics.

RESULTS AND DISCUSSION

Figure 2 is a plot of the time (2.5 minutes for each scan) scans of the water vapor absorption at several water vapor pressures at a fixed frequency 1002.0 cm^{-1} . The pathlength was 80.1 m and the temperature was $337 \pm 2 \text{ K}$. A fixed frequency operation was achieved by setting the diode laser at a fixed dc current and the cryogenic cooler at a fixed temperature. The frequency 1002.0 cm^{-1} is one of a number of frequencies in the $10 \mu\text{m}$ region at which there are no nearby strong water vapor absorption lines. Therefore, the observed absorption at the operating pressures is essentially the continuum type. As shown in each scan, there are some minor fluctuations which we attribute to very minute temporal temperature fluctuations; the stated temperature uncertainty of two degree centigrades is spatial rather than temporal.

Figure 3 is a plot of the water vapor continuum absorbance αL vs. the square of the water vapor pressure for each of the five scans shown in Fig. 2, αL being equal to $-\ln T_r$, where T_r is the transmittance. The solid straight line represents the calculated values using an empirical formula for continuum

center the continuum absorption as obtained by nonlinear least squares method does not vary as rapidly as the square of the water vapor pressure. At the present, there is no adequate reason to account for this finding.

CONCLUSION

We have performed high resolution diode laser absorption measurements for both water vapor line and continuum absorption in selected region near $10\mu\text{m}$ using a moderately long pathlength both at room and at slightly elevated temperatures. Our measurement results are in reasonable good agreement with previous results at room temperature. At higher temperatures, our observed continuum absorption coefficient is somewhat higher implying a weaker temperature dependence. An extension of this type of measurements will undoubtedly aid further understanding of the continuum absorption characteristics.

ACKNOWLEDGEMENT

The authors would like to thank Dr. K. J. Linden for supplying the diode lasers and Dr. C. S. Venkatesh and Mr. W. Towne for their helpful discussion and assistance respectively. They are grateful to Dr. S. A. Clough for his encouragement and support for this program.

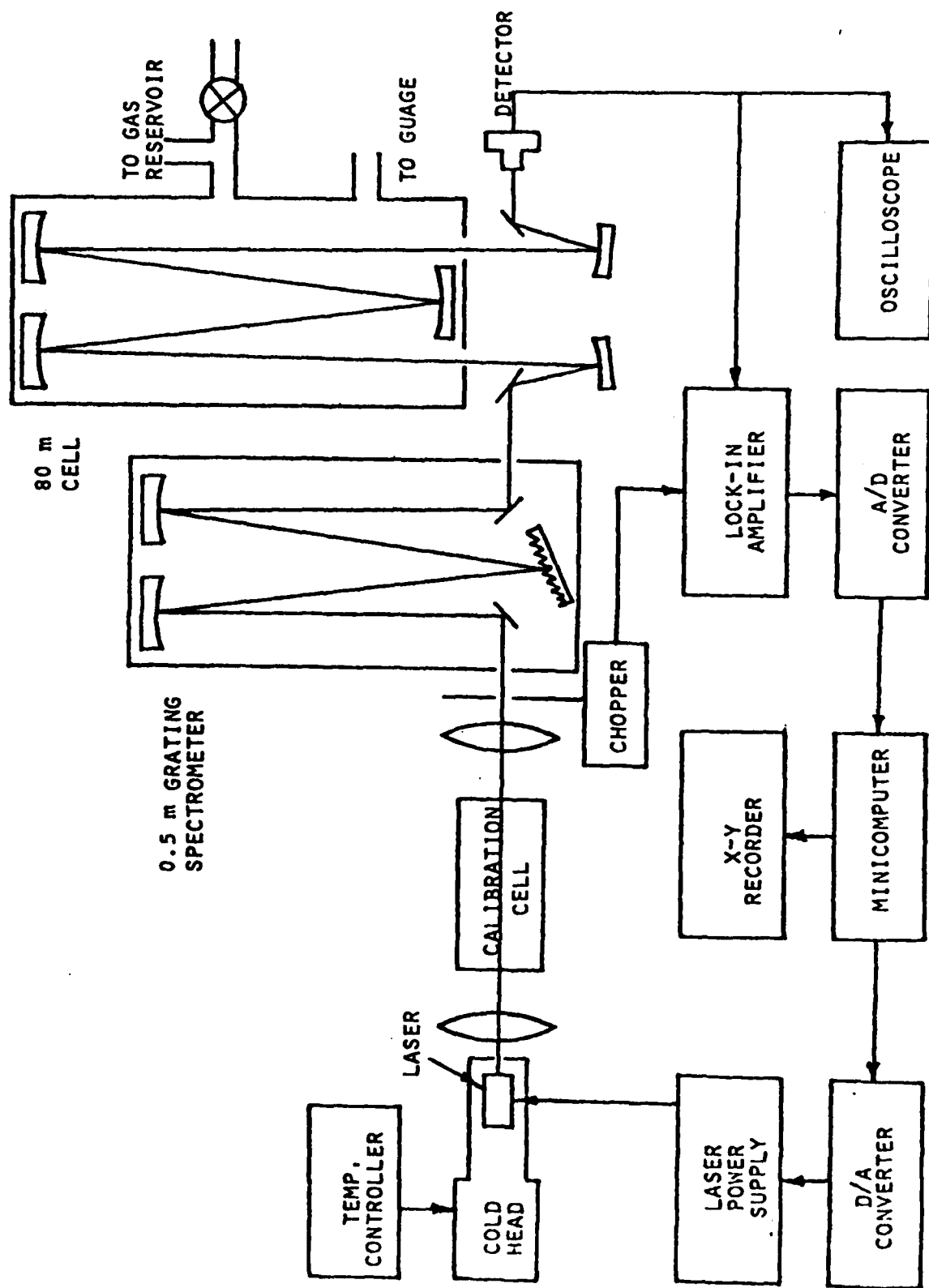
REFERENCES

1. K. J. Bignell, F. Saiedy, and P. A. Sheppard, J. Opt. Soc. Am., 53, 466 (1963).
2. P. Varanasi, S. Chou, and S. S. Penner, J. Quant. Spectrosc. Radiat. Transfer, 8, 1537 (1968).
3. K. J. Bignell, Q. J. R. Meteorol. Soc. 96, 390 (1970).
4. D. E. Burch, "Investigation of the Absorption of Infrared Radiation by Atmospheric Gases," Semiannual Technical Report, Aeronutronic Division, Philco Ford Corporation, Aeronutronic Report U-4784 (30 January 1971).
5. D. E. Burch, D. A. Gryvnak, and J. D. Pembroke, "Investigation of the Absorption of Infrared Radiation by Atmospheric Gases: Water, Nitrogen, Nitrous Oxide," AFCRL-71-0124 (1971).
6. J. H. McCoy, D. B. Rensch, and R. K. Long, Appl. Opt. 8, 1471 (1969).
7. V. N. Arefev, V. I. Dianov-Klovov, V. F. Radionov and N. I. Sizov, Opt. Spectrosc., 39, 560 (1975).
8. K. G. White, W. R. Watkins, C. W. Bruce, R. E. Meredith, and F. G. Smith, Appl. Opt. 17, 2711 (1978).
9. E. K. Damon, J. C. Peterson, F. S. Mills, and R. K. Long, "Spectrophone Measurement of the Water Vapor Continuum at DF Laser Frequencies," RADC-TR-75-203 (1975), OSU Report ESL 4045-1.
10. M. S. Shumate, R. T. Menzies, J. S. Margolis, and L-G. Rosengren, Appl. Opt. 15, 2480 (1976).
11. Felix Franks, Ed., "Water: A Comprehensive Treatise," in The Physics and Physical Chemistry of Water (Plenum, New York, 1972), Vol. 1.
12. J. H. Van Vleck and V. Weisskopf, Rev. Mod. Phys. 17, 227 (1945).
13. G. Birnbaum, J. Quant. Spectrosc. Radiat. Transfer, 21, 597 (1979).
14. W. C. Braun, and H. Leidecker, J. Chem. Phys. 61, 3104 (1974).
15. S. A. Clough, F. X. Kneizys and R. W. Davies, Private Communications.
16. D. E. Burch, D. A. Gryvnak, and F. J. Gates, "Continuum Absorption by H₂O Between 330 and 825 cm⁻¹," Final Report for Period 16 October 1973-30 September 1974, Aeronutronic Division, Philco Ford Corporation, AFCRL-TR-74-0377 (September 1974).

17. R. S. Eng and A. W. Mantz, J. Mol. Spectrosc. 74, 388 (1979).
18. R. W. Davies and B. A. Oli, J. Quant. Spectrosc. Radiat. Transfer, 20, 95 (1978).
19. C. Camy-Peyret and J.-M. Flaud, Mol. Phys., 32, 523 (1976).
20. J.-M. Flaud, C. Camy-Peyret and J.-P. Maillard, Mol. Phys., 32, 499 (1976).
21. R. S. Eng, P. L. Kelley, A. Mooradian, A. R. Calawa, and T. C. Harman, Chem. Phys. Lett. 19, 524-528 (1973).
22. G. P. Montgomery, Jr., Appl. Opt. 17, 2299 (1978).
23. R. E. Roberts, J. E. A. Selby, and L. M. Biberman, Appl. Opt. 15, 2085 (1976).
24. J. E. A. Selby, E. P. Shettle, and R. A. McClatchey, "Atmospheric Transmittance from 0.25 to 28.5 μ m: Supplement LOWTRAN 3B (1976)" AFGL-TR-76-0258 ERP 587 (7 November 1976).

FIGURE CAPTIONS

- Fig. 1 Schematic diagram of the experimental setup for water vapor continuum absorption measurements.
- Fig. 2 Water vapor continuum absorption at 1002.00 cm^{-1} at 337K and 80.1m pathlength for different water vapor pressures.
- Fig. 3 Water vapor continuum absorbance (αL) vs. water vapor pressure squared at 1002.00 cm^{-1} and 337K. Solid curve is calculated using a formula from Ref. 24.
- Fig. 4 Water vapor continuum absorbance (αL) vs. water vapor pressure squared at 1002.00 cm^{-1} and 296K. Solid curve is calculated using a formula from Ref. 24.
- Fig. 5 Water vapor continuum and line absorption near 1014.45 cm^{-1} for an 80.1m pathlength, 337K cell temperature and 58.9 Torr of H_2O vapor pressure. Solid and dotted curves represent observed and nonlinear least squares fitted values respectively.
- Fig. 6 Water vapor continuum absorption frequency at 296K. Solid curve is calculated using a LOWTRAN 3B formula. (see Ref. 24)
- Fig. 7 Water vapor continuum absorption vs. frequency at 337K. Solid curve is calculated using a LOWTRAN 3B formula. (see Ref. 24)



SCHEMATIC DIAGRAM OF EXPERIMENTAL SETUP

Fig. 1

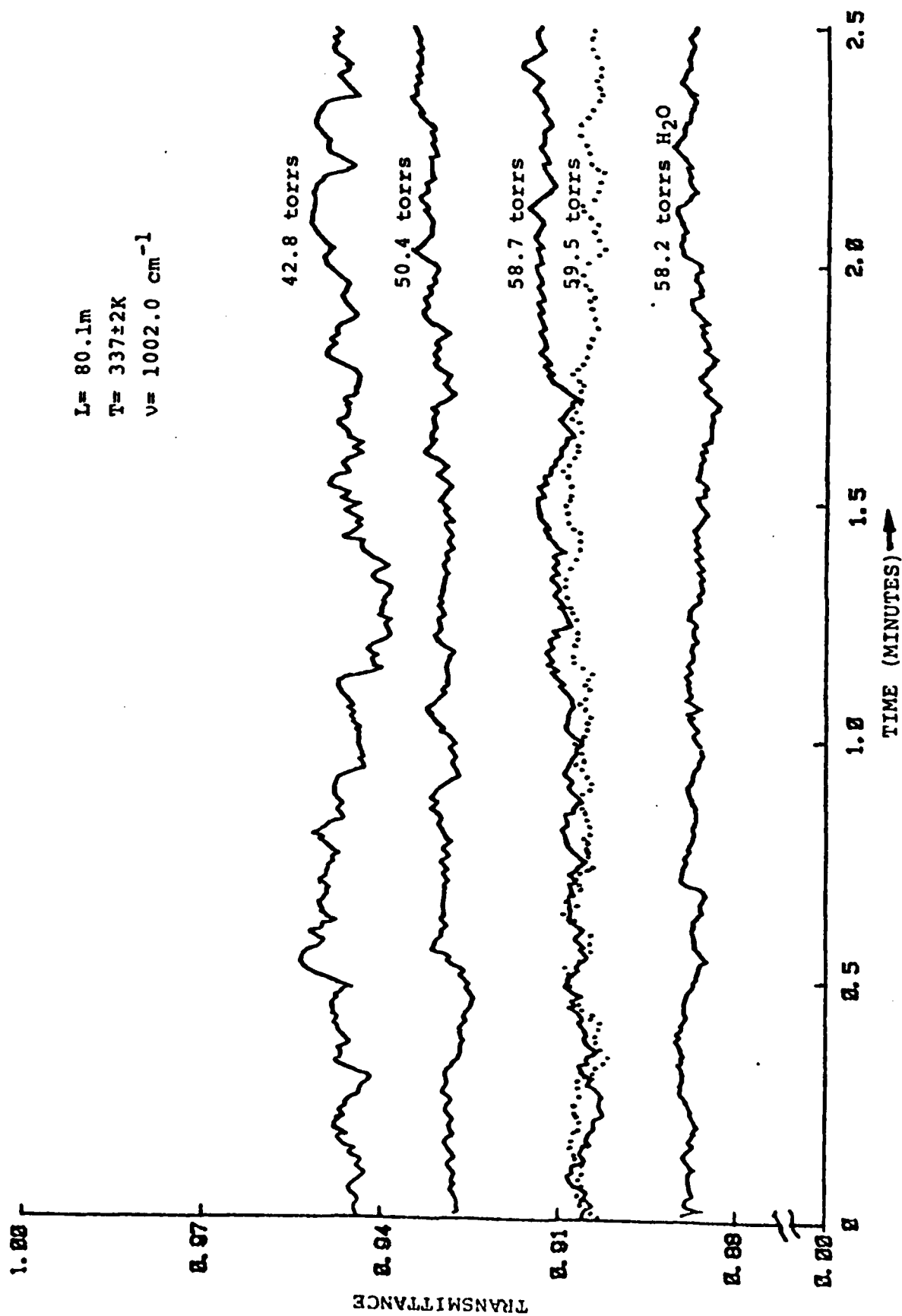


Fig. 2

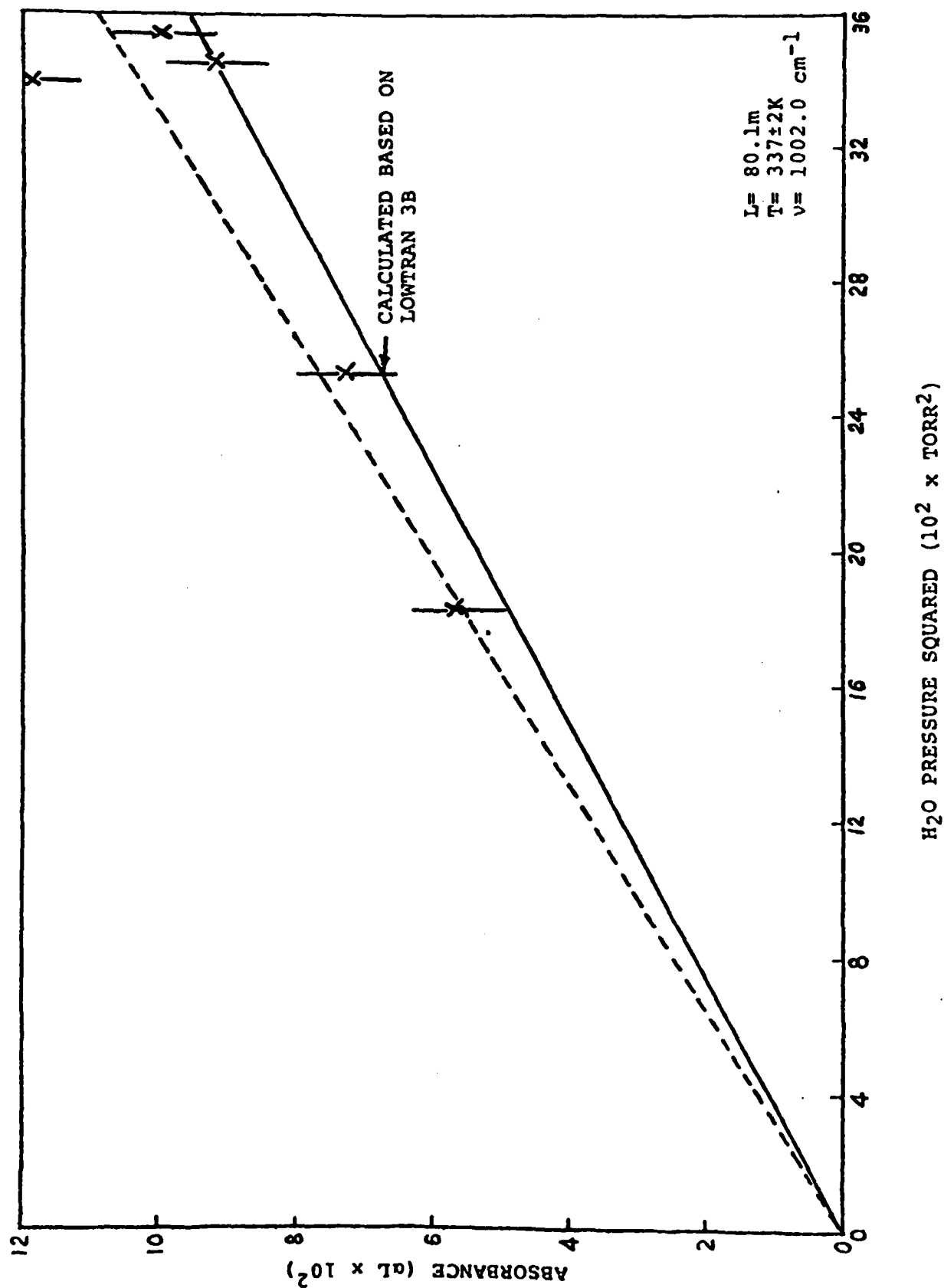


Fig. 3

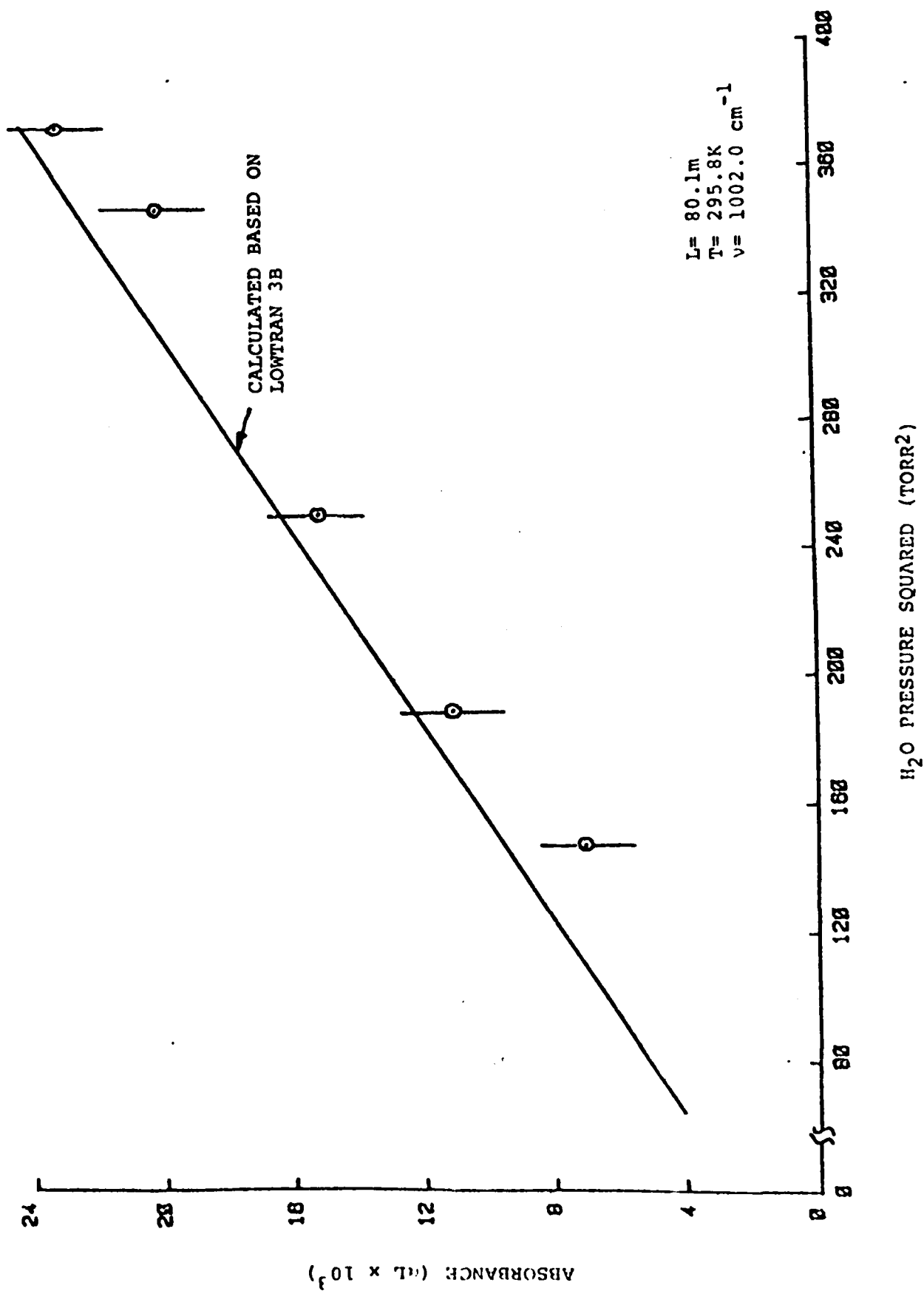
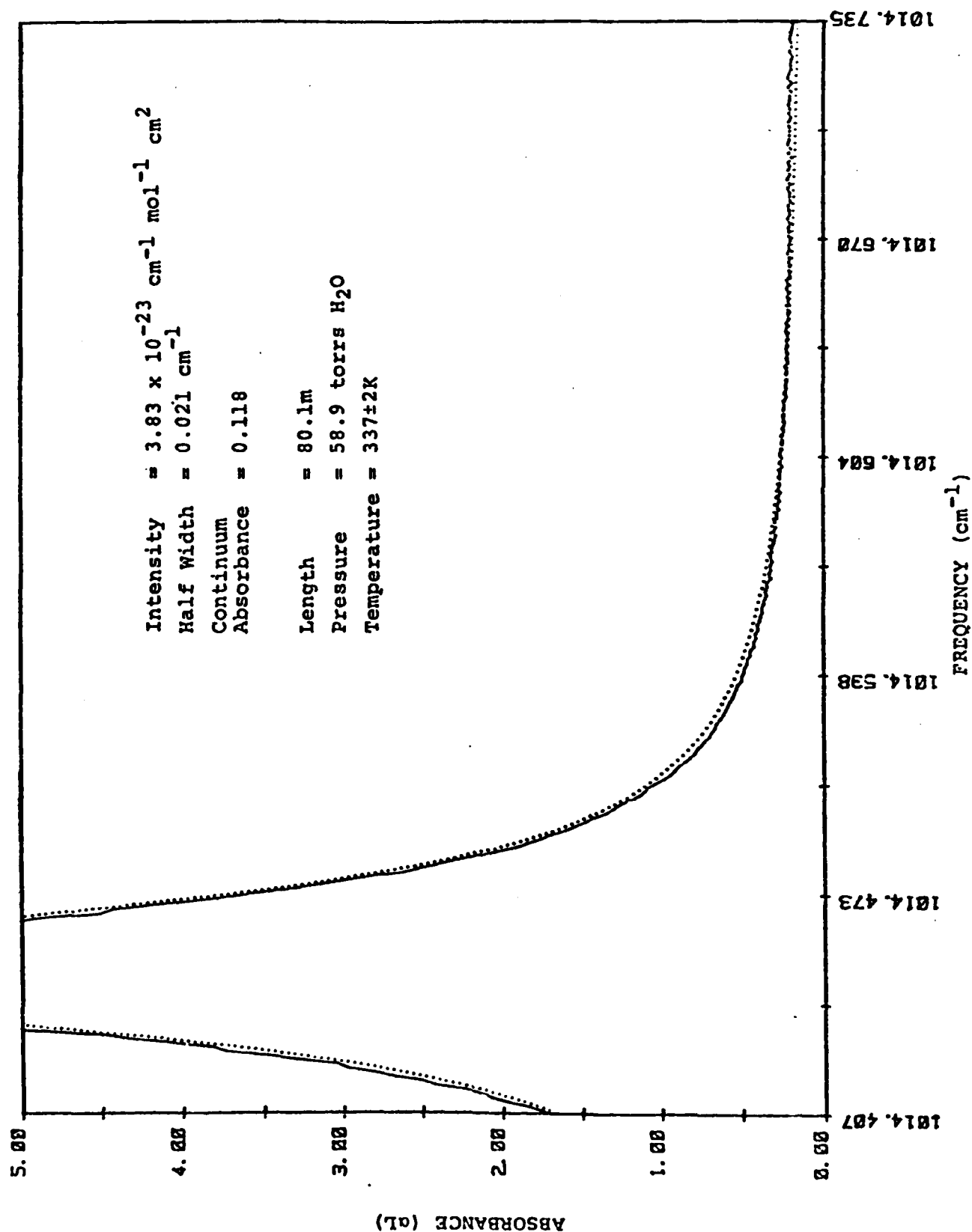


Fig. 4

Fig. 5



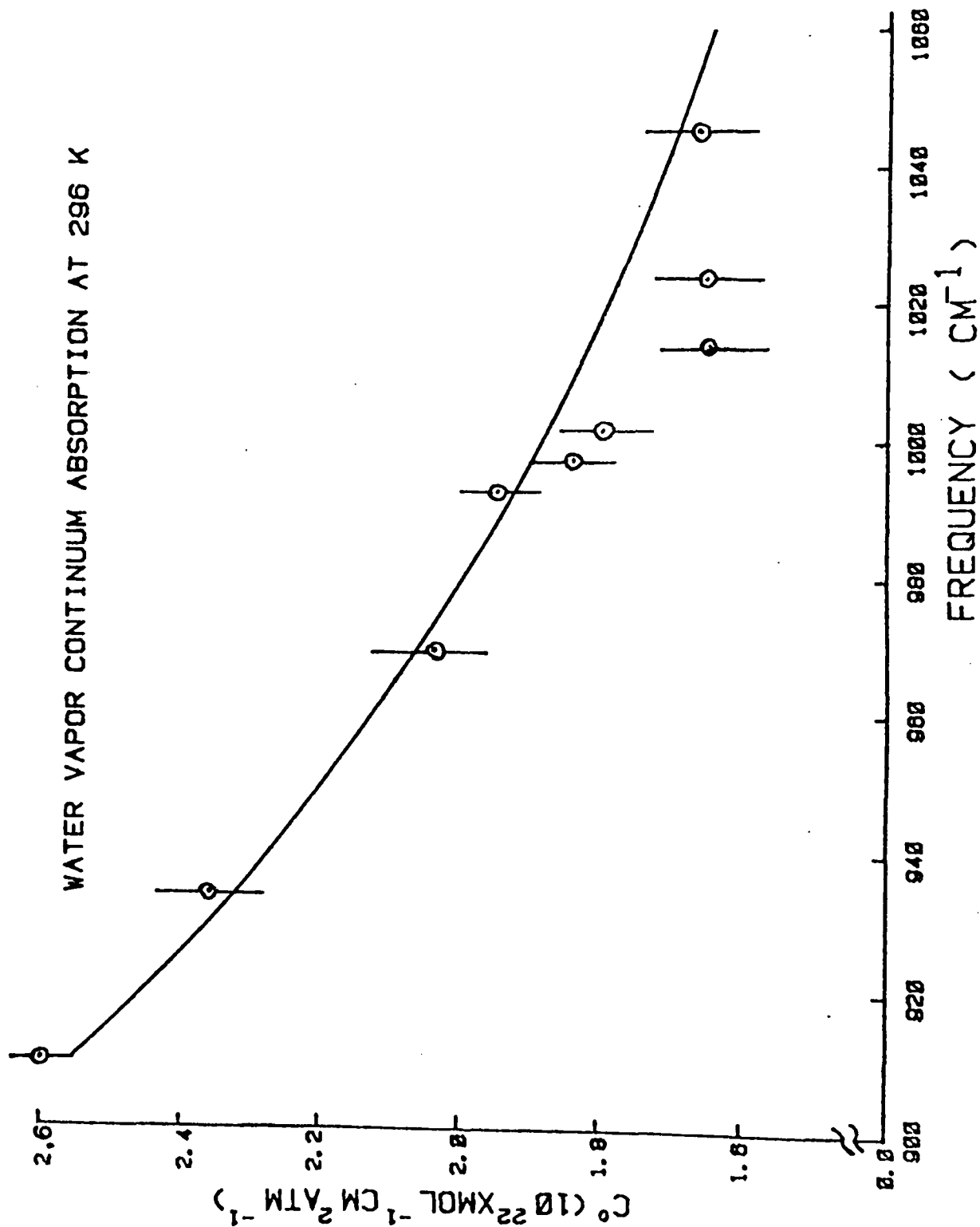


Fig. 6

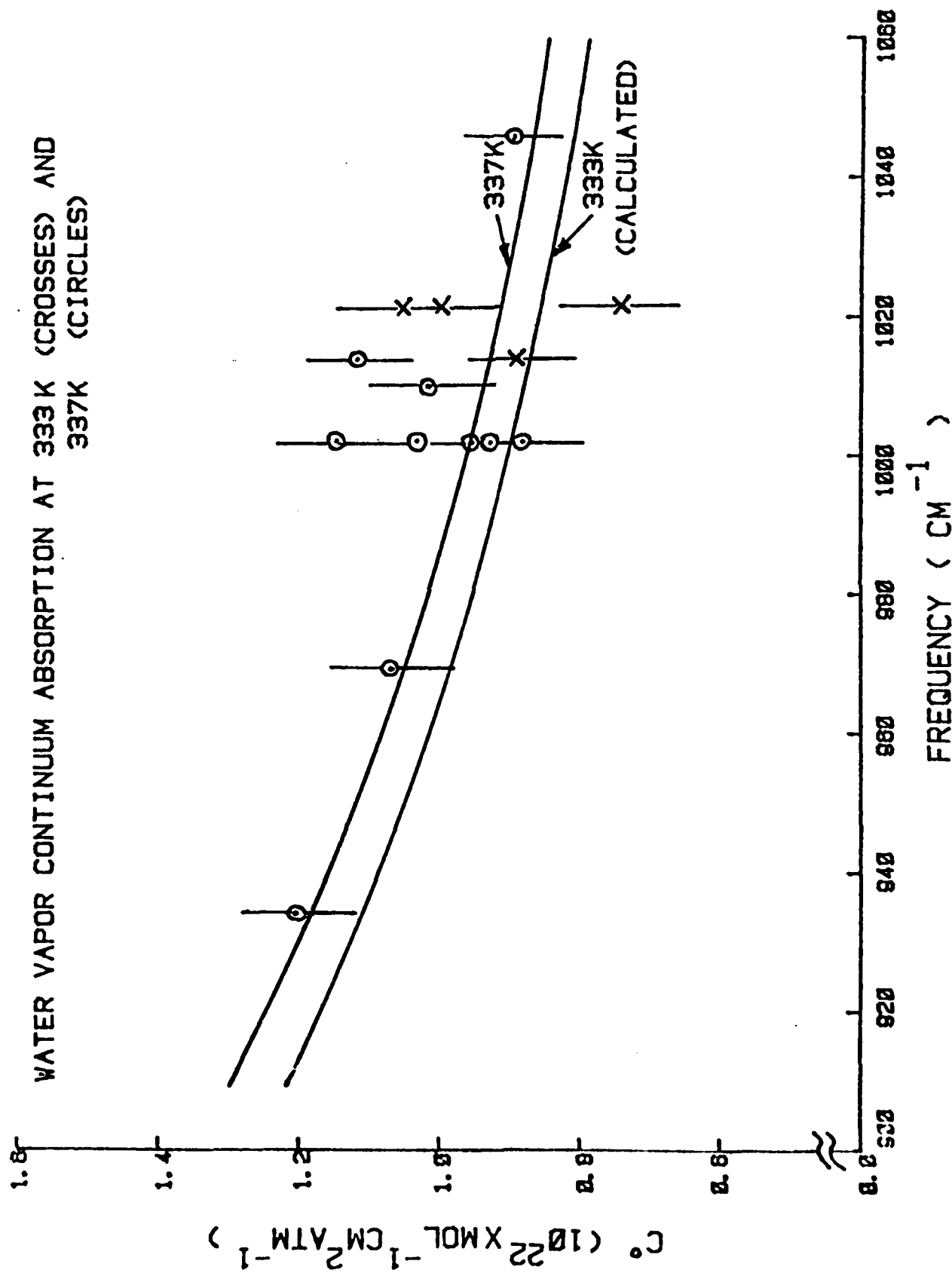


Fig. 7

5.0

THEORETICAL FEASIBILITY STUDY OF WATER VAPOR LINESHAPE BY
DOUBLE RESONANCE SPECTROSCOPY

R. S. Eng, A. W. Mantz and C. G. Venkatesh

Laser Analytics, Inc.
25 Wiggins Avenue
Bedford, MA 01730

ABSTRACT

A proposed double resonance spectroscopic technique is described in which a CO laser in coincidence with a water vapor line is used to pump the water vapor transition and a CW Tunable Diode Laser is used to probe the water vapor absorption coefficient up to 100 halfwidths from the pressure broadened line to determine the lineshape.

FEASIBILITY STUDY OF PRESSURE-BROADENED
RO-VIBRATIONAL SPECTRAL CONTOURS
BY NON LINEAR SPECTROSCOPY

1.0 OBJECTIVE

To map and study individual collision broadened, ro-vibrational contours of H₂O vapor as far as 100 half widths ($\Delta\nu_{1/2}$) away from line center. The basic idea, experimentally, is to probe the wings by using a tunable diode laser to monitor absorption changes caused along the whole contour by a strong pump at line center. The pump laser is to be suitable modulated to achieve high sensitivities.

[A very important assumption implicit in this report is the existence of rotational equilibrium in the system at all times. This is believed to be a justifiable assumption, considering the rapidity of rotational relaxation.]

2.0 FEASIBILITY ANALYSIS

2.1 INTRODUCTION

The principal questions considered are the following, in order of priority.

a. In case the pump pulse is short (in time), will its pulse width be long enough for the pressure broadening to be seen? In other words, is the average "dephasing" or collision time short enough so that a sufficient number of collisions can occur during the pulse to give a distortionless pressure-broadened contour?

b. What are reasonable estimates for the changes (in magnitude and time) produced at the "probe" points when saturation occurs at the "pump" point?

c. In view of the results from a and b, what specifically would be the range of relevant parameters to be considered for pumping H₂O?

d. Taking into account the results in c, what would be the general experimental setup, using conservative estimates of instrument performances, to make the measurements?

2.2 THEORETICAL CONSIDERATIONS

As will be seen later, the 1923.16 cm⁻¹ line [(010)7_{4,3}+ (000)6_{3,4}] is one of the few (in H₂O) that can be easily saturated. Hence, where necessary, data for this line has been used. Other than its spectral suitability, there is nothing atypical about the line so the results are of general applicability.

a. In a gas mixture (containing only 2 gases, say, types a and b) the collision frequency per molecule per unit vol.¹

$$\frac{1}{\tau_{a,b}} = N_{b,a} Q_{ab} \sqrt{\frac{8kT}{\pi\mu}}$$

$$\frac{1}{\tau_{a,a} \quad (b,b)} = \frac{2N_a}{(N_b)} \cdot \frac{Q_{aa}}{(Q_{bb})} \sqrt{\frac{8kT}{\pi M_a} \quad (M_b)}$$

$$N_{a,b} = \# \text{ molecules of type } a,b \text{ cm}^{-3}$$

$$Q = \text{collision cross-section} = \pi \sigma^2 \quad (\sigma = \text{molecular radius})$$

For water vapor (type a) at a partial pressure of ~10 torr in a mixture with N_2 (type b) at a partial pressure ~750 torr.

$$N_b = 24.4539 \times 10^{18} \text{ molecules cm}^{-3}$$

$$Q_{H_2O-H_2O} \approx Q_{N_2-H_2O} \approx \pi \left(\frac{\sigma_{N_2} + \sigma_{H_2O}}{2} \right)^2 \pi \times (1.5 \text{ \AA})^2 =$$

$$\pi \times (1.5)^2 \times 10^{-16} \text{ cm}^2$$

$$k(\text{Boltzmann's const}) = 1.3805 \times 10^{-16} \text{ erg } ^\circ\text{K}^{-1}$$

$$\left. \begin{array}{l} M_{N_2} \approx 28 \\ M_{H_2O} \approx 18 \end{array} \right\} \text{ in a.m.u. } 1 \text{ a.m.u.} = 1.6605 \times 10^{-24} \text{ gm}$$

$$T \approx 300^\circ\text{K}$$

$$\therefore \frac{1}{\tau_{H_2O-N_2}} \approx 3.7 \times 10^9 \text{ sec}^{-1}$$

$$\left(\frac{1}{\tau_{H_2O-H_2O}} \approx 5 \times 10^7 \text{ sec}^{-1} \right)$$

Collision times are of the order of 10^{-9} secs, whereas anticipated pulse widths are $\approx 10^{-6}$ secs. Hence this is not a limiting factor.

b. Saturation effects are expected to be different for homogeneously-broadened contours as compared with inhomogeneously (Doppler)-broadened ones.

For Doppler-broadened contours, if saturation occurs at one point there is an overall but only slight pulldown of the population vs. velocity distribution, the disturbance being felt essentially near (within $\Delta v_{1/2}$) the saturation point.⁵ An intuitive explanation for this phenomenon would be that Doppler-broadening is due to the division of molecules into different classes, according to their axial velocities. Hence, a hole burnt into one of them disturbs the equilibrium and the other molecules, by cross-relaxation, feed into this hole, causing a net pulldown of the velocity distribution contour. Translational energy transfer is expected to be very efficient for small changes in energy, hence the changes are significant only near the hole. So, for a Doppler-broadened contour, one has to probe within a $\Delta v_{1/2}$ of the exciting line to see any changes. For a homogeneously-broadened line, such restrictions should not exist, since in principle, a significant change in population at any point of the contour should have the same effect all along it. This means one could saturate at line center and probe say 50 or even 100 $\Delta v_{1/2}$ away and still be able to see significant changes in absorption. However, at 50 or 100 $\Delta v_{1/2}$ away one could get interferences from the overlapping of other contours, and total absorption change would then be due to the cumulative effect of all the overlapping points. In the absence of serious interferences, suitable curve fitting should yield the shape of the contour.

The following calculation assumes (as a first approximation) a square 'pump' pulse and a 2 level-system.

_____ 2 (initially pumped level)
 _____ 1 (ground state)

Let $N_1(t)$, $N_2(t)$ be the population densities (as a function of time) of levels 1,2. Let $W(\nu) = W_{12}(\nu) = W_{21}(\nu)$ be the induced transition rate between levels 1 and 2, " t_2 " the composite relaxation time from 2 \rightarrow 1 and " t_s " the spontaneous lifetime of 2. The rate equations are:

$$\frac{dN_2}{dt} = -\frac{N_2}{t_2} - (N_2 - N_1) W(\nu)$$

$$\frac{dN_1}{dt} = \frac{N_2}{t_s} + (N_2 - N_1) W(\nu)$$

These are a set of coupled, first order, linear differential equations, with constant coefficients. Solving them by standard Laplace transform techniques, we get for the change in population of 1.

$$\frac{N_2(t)}{N_1(0)} = \frac{[e^{-a_1 t} - e^{-a_2 t}]}{(a_2 - a_1)} \cdot W$$

$$a_1 = \frac{(2W + 1/t_2) - \sqrt{(2W + 1/t_2)^2 - 4W(1/t_2 - 1/t_s)}}{2}$$

$$a_2 = \frac{(2W + 1/t_2) + \sqrt{(2W + 1/t_2)^2 - 4W(1/t_2 - 1/t_s)}}{2}$$

At pressures of ~1 atmosphere, t_2 is of the order of 10^{-7} to 10^{-9} secs. whereas t_s is of the order of 10^{-2} to 10^{-3} secs. (~17 . 4 x 10^{-3} secs. for the 1923.16 cm^{-1} line) so $1/t_s$ can be neglected in comparison to $1/t_2$. (See appendix) Physically this makes sense, since in the high pressure region, where natural line widths are totally insignificant, the effects of t_s should be ignorable. Therefore,

$$a_1 = \frac{(2W + 1/t_2) - \sqrt{4W^2 + (1/t_2)^2}}{2}$$

$$a_2 = \frac{(2W + 1/t_2) + \sqrt{4W^2 + (1/t_2)^2}}{2}$$

Since we are interested in the optimum pulse widths, the times at which $N_2(t)/N_1(0)$ is a maximum has to be estimated. Setting $dN_2(t)/dt = 0$,

$$0 = \frac{1}{N_1(0)} \frac{d}{dt} N_2(t) = \frac{W}{a_2 - a_1} \left[-a_1 e^{-a_1 t_{\max}} + a_2 e^{-a_2 t_{\max}} \right]$$

or

$$a_1 e^{-a_1 t_{\max}} = a_2 e^{-a_2 t_{\max}}$$

therefore,

$$t_{\max} = \left(\frac{\ln a_2 - \ln a_1}{a_2 - a_1} \right)$$

Hence t_{\max} should be the best value for the pulse width of the pump lasers.

Table I gives the various parameters for a range of relaxation times t_2 and pump laser intensities I_v . Table II indicates the changes in intensity to be expected for the probe beam for a range of partial pressure x path lengths for H_2O . Figure 1 sketches the kinetics of the pumping process for $t_2 = 10^{-7}$ secs and $I_v = 1 \text{ kW/cm}^2$. (See appendices for details of the calculation of $t_{\text{spontaneous}}$ and $W_{(v)}$).

c. Four important feasibility parameters are estimated in the following paragraphs.

(i) A cursory examination of the band origins will indicate that one is restricted to the v_2 band fundamental region ($\sim 1595 \text{ cm}^{-1}$) since there are no easily accessible and intense enough IR sources in the v_3 , v_1 , and $2v_2$ regions (~ 3756 , ~ 3657 and $\sim 3152 \text{ cm}^{-1}$). Also, unfortunately, all the intense water vapor laser lines correspond to ro-vibrational transitions between 100 and 020 or 001 and 020 or pure rotational transitions between levels in 100, 001 or 020⁶. None of these would deplete the ground state populations. Hence, the only readily available pump source would be a Q-switched CO laser. The 1923.16 line is chosen since it has a high value of line strength⁴ and is in near coincidence with the 1923.15 cm^{-1} line of the CO laser. (Additional CO laser lines would also enhance the pumping effect.)

(ii) A reasonable estimate of intensity from a focussed Q-switched CO laser is $\sim 1 \text{ kW cm}^{-2}$. The other crucial quantity is the relaxation time for transitions in v_2 (010). This important and useful information is found in the work of Finzi et. al,⁷ who have obtained self relaxation rates for v_1 , v_3 , and $2v_2$ and cross-relaxation rates for v_1 , v_3 , and $2v_2$ due to foreign gases like Ar, O_2 and N_2 .

In the 10 Torr H_2O -750 Torr N_2 mixture, the self deactivation probability for the v_2 fundamental is ~ 0.5 (the worst

case); i.e., one out of 2 collisions relaxes the molecule. Even at such a high deactivation rate, the relaxation time is $0.5 \times 1/\tau_{\text{H}_2\text{O}-\text{H}_2\text{O}} = (0.5 \times 5 \times 10^7)^{-1} \approx 40$ nanoseconds.

The $\text{H}_2\text{O}-\text{N}_2$ deactivation probability (inferred from the values for v_1, v_3) is $\sim 10^{-3}$. Hence, the relaxation time due to collisional deactivation by $\text{N}_2 \approx (10^{-3} \times 3.7 \times 10^9)^{-1} = 2.7 \times 10^{-7} \approx 270$ nanoseconds. So the water self-deactivation rate is the controlling factor.

Now 40 nanoseconds is well within the resolution time of commercially available signal avergers like the boxcar.

(iii) We now consider the smallest change in absorption ($\Delta\alpha L$) caused by the pump and the possibility of detecting it. As mentioned before, reasonable values for laser power and relaxation times t_2 are $\sim 1 \text{ kW cm}^{-2}$ and $10^{-7} \rightarrow 10^{-8}$ secs, respectively.

The αL caused in the probe beam by ~ 10 Torr H_2O and a 100 cm path length is 5.4×10^{-4} about $50 \Delta\nu_{1/2}$ away from line center (Table II). The % change in population caused by the pump would be $\sim 10\%$ (Table I). The total change in ' αL ' ($\Delta\alpha L$) i.e., the signal to be detected $\approx 0.1 \times 5.4 \times 10^{-4} \approx \underline{\underline{5 \times 10^{-5}}}$ so the range of $\Delta\alpha L$ would be part in $10^{-4}-10^{-5}$.

(N.B. There is no possibility of greatly exceeding a partial pressure of ~ 10 Torr of H_2O at 296°K since the saturated vapor pressure is ~ 20 Torr and above this value, condensation would occur on the windows of the sample cell.)

A discussion of detectable signal levels in the presence of noise is given in section d.

(iv) Now consider the interferences from other lines in the region of $\sim 50 \Delta\nu_{1/2}$ (3 cm^{-3}) from line center. The AFCRL data⁴ show that on the low wavenumber side there are two lines at

918.05 cm^{-1} and 1921.33 cm^{-1} of comparable strength that could seriously interfere with the probed contour. However, in the longer wavenumber region, most of the lines are of strengths at least 1000 times smaller than the one at 1923.156 cm^{-1} . So this region should be relatively interference free. In the absence of any serious asymmetry effects, mapping half the contour would enable one to extend it to the other half.

d. Experimental. Having discussed the theoretical calculations, we turn our attention to the experimental part of the program. Figure 1 is a block diagram showing the main equipment for measuring the lineshape of the pressure broadened H_2O line at 1923.160 cm^{-1} .

For convenience of discussion, the equipment can be divided into four functional groups--namely, the pump, the tunable probe, the interaction cell, and the analyzer. The pump consists of the following components, a grating-controlled, Q-switched CO laser and its high voltage power supply, gas handling apparatus needed to fill the CO laser and a constant control unit to keep the discharge wall at about -80°C . A beam expander and shaper produce a sheet beam. The tunable probe system consists of a tunable diode laser, a laser current control module, a cryogenic cooler for the diode mount, a temperature controller for the cooler, and focussing optics to form a small circular beam for the multipass cell in which the beam is small and the beam images are confined to one row instead of the usual two. The cell accepts the sheet beam of the CO laser pump and the probe beam from the diode laser. The sheet beam is perpendicular to the probe beam and traverses the cell only once while the diode laser beam is made to traverse the cell many times. The analyzer consists of collecting optics for the diode laser beam, a diode mode filtering spectrometer, a high-speed detector, a boxcar amplifier, an X-Y recorder and a pulse digitizer for more accurate analysis of the pulse signal. The absorber is used to absorb the entire CO laser signal and prevent CO pump power from falling on the collecting optics.

The following is a detailed description of the four groups.

1. The Pump The CO laser is to have a plasma discharge tube filled with CO, He and N₂ at a total pressure of about 20 to 30 torr. The partial pressures will be adjusted to maximize the power output for the 7-6 band P(16) line. For a plasma tube approximately 1.2 m long with a 10 mm bore, a 15 kV high voltage power supply is necessary to drive 20 mA through the discharge bore and to provide a ballast drop of about 6 kV. The plasma tube has Brewster windows of either CdTe or ZnSe.

The cavity Q-switching is implemented by a rotating mirror on the axis of plasma tube. The reflected beam from the rotating mirror directed toward a diffraction grating which is Littrow mounted for CO line selection.

The output of the CO laser is expanded to about 2.5 cm diameter using a telescope beam expander. The expanded beam is then focussed down to about 0.200 mm in one dimension by a cylindrical lens. The peak power density is about 2 kW/cm^2 for 100 Watts peak power. This power density can be maintained approximately over a length of about $\frac{2\pi}{\lambda} W_0^2$, where W_0 is the radius of the beam waist. For $W_0 = 100 \text{ } \mu\text{m}$, the length is approximately 1.2 cm.

2. The Tunable Probe The tunable diode laser and its current and temperature controlling equipment belong to a commercial system, Laser Analytics Model LS-3, needing very little modification. The focussing optics

should be capable of focussing down the laser beam diameter to about 0.200 mm in diameter. The diode laser beam entering the field mirror of the multiple-pass cell has this diameter. It expands to a larger size as it travels toward one of the objective mirrors. The axis of the diode laser beam is perpendicular to the axis of the CO laser beam and they lie in the plane of the CO laser sheet beam as shown in Figure 2.

3. The Interaction Cell The cell is a regular White type with the field mirror designed so that all images on the field mirror are in one row instead of two. Since the pump beam has a thickness of 0.2 mm and a length of 1 cm and a width of about 2.5 cm; the diode laser beam must be confined to this volume in order to take advantage of the high pump power density. To obtain a multiple-pass length of 1 m of pumped path (assuming 100 passes), requires that each pass should be 1 cm long. Due to diffraction, 1 cm is about the axial length the beam can maintain its small diameter of 0.2 mm. The radius of curvature of the White cell is about 10 cm and the objective mirrors are 1 cm in diameter.
4. The Analyzer The collecting optics collect the diode laser signal and focusses it on the entrance slit of a grating spectrometer for diode laser mode separation. The output of the spectrometer is detected by a high-speed detector. A photovoltaic InSb, detector with a rise time about 1 ns should be adequate. The box-car amplifier averages the diode laser signal during the pump pulse duration in which the diode laser beam attains a slightly higher transmission limited by the relaxation time in the upper level of the H₂O transi-

tion, t_2 . The pulse digitizer allows one to perform more accurate analysis of the pulse shape. The X-Y recorder is used to display the boxcar amplifier output. Because the H_2O line is very intense, purging is required along both the CO laser and diode laser beam paths. This adds to the overall complexity of the experiment.

Based on existing literature on Stark spectroscopy, 1 part in 10^6 detection of the transmitted probe signal is possible for a very clean probe beam such as that of a gas laser. With the diode laser, it has been shown that a signal-to-noise of better than one part in 10^5 is attainable. Therefore, it is not unreasonable to expect that a detection of one part in 10^5 is possible with the diode laser as a probe.

e. The main advantage of this method over conventional absorption techniques is that it is much more sensitive. Herein lies the potential of being able to extend one's measurement to 50 or even $100 \Delta\nu_{1/2}$ away from line center. The sensitivity is due to the fact that we are modulating the system of molecules (almost noise free) instead of just the source (which would modulate also the source noise). This enables us to pull out the signal buried in noise.

Comparable sensitivities by conventional methods would be achieved only by using path lengths of ~1 km, which in turn compounds the experimental problems, necessitating critical construction and alignment of a long multipass cell, among others.

It must be noted, in conclusion, that the technique does not (in this case) eliminate interferences from strong neighboring lines. It is not a panacea in the sense that only one line

is modulated separating it from the others. This is because there is rotational equilibrium at all times, so pumping one line disturbs other lines connected to the same vibrational band. However, if a suitable molecular system is chosen in which two overlapping unconnected transitions are to be spectrally separated, then this technique is ideally suited for such applications. Also, in the absence of too much spectral overlap, entire contours $\sim 50 \Delta\nu_{1/2}$ can be mapped, helping to resolve the long standing controversy as to whether at large $\Delta\nu_{1/2}$ the homogenously broadened lineshape is still Lorentzian.

TABLE I

Relaxation Time " τ_2 " In Secs	$I_v = 10 \text{ KW cm}^{-2}$ ($W = 4 \cdot 4 \times 10^7$)		$I_v = 1 \text{ KW cm}^{-2}$ ($W = 4 \cdot 4 \times 10^6$)		$I_v = 100 \text{ Watts cm}^{-2}$ ($W = 4 \cdot 4 \times 10^5$)		$I_v = 10 \text{ Watts cm}^{-2}$ ($W = 4 \cdot 4 \times 10^4$)		$I_v = 1 \text{ Watt cm}^{-2}$ ($W = 4 \cdot 4 \times 10^3$)	
	$t_{\max} \text{ (secs)}$	$100 \times \frac{N_2(t)}{N_1(o)}$	$t_{\max} \text{ (secs)}$	$100 \times \frac{N_2(t)}{N_1(o)}$	$t_{\max} \text{ (secs)}$	$100 \times \frac{N_2(t)}{N_1(o)}$	$t_{\max} \text{ (secs)}$	$100 \times \frac{N_2(t)}{N_1(o)}$	$t_{\max} \text{ (secs)}$	$100 \times \frac{N_2(t)}{N_1(o)}$
10^{-9}	3.2×10^{-9}	3.68	5.4×10^{-9}	0.43	7.7×10^{-9}	0.04	1×10^{-8}	0.004	1.2×10^{-8}	0.0004
10^{-8}	1.3×10^{-8}	19.04	3.2×10^{-8}	3.68	5.4×10^{-8}	0.43	7.7×10^{-8}	0.04	1×10^{-7}	0.004
10^{-7}	3.7×10^{-8}	40.2	1.3×10^{-7}	19.04	3.2×10^{-7}	3.7	5.4×10^{-7}	0.43	7.7×10^{-7}	0.04
10^{-6}	5.9×10^{-8}	48.3	3.4×10^{-7}	40.2	1.3×10^{-6}	19.04	3.2×10^{-6}	3.7	5.4×10^{-6}	0.43

TABLE II

LINE STRENGTH 'S' FOR THE 1923.16 cm^{-1} LINE = $1.04 \times 10^{-20} \Delta\nu_{1/2} = 0.078 \text{ cm}^{-1}$

$$I = I_0 e^{-\alpha L}, \alpha = S \cdot g(\nu) \cdot N \quad (N = \# \text{ of molecules } \text{cm}^{-3})$$

(Partial pr. of water 'P') x (Path length 'L') Range of P = 10-100 Torr L = 10-100 cms	Probe point in terms of $\Delta\nu_{1/2}$ in away from line center	Lorentzian Lineshape function $g(\nu)$	αL
100	0	4.08	0.14
	10	0.0373	0.0013
	20	0.0093	0.00031
	50	0.0016	0.000054
	100	0.0004	0.000013
500	0	4.08	0.68
	10	0.0373	0.0062
	20	0.0093	0.0015
	50	0.0016	0.00027
	100	0.0004	0.00007
1,000	0	4.08	1.37
	10	0.0373	0.012
	20	0.0093	0.003
	50	0.0016	0.00054
	100	0.0004	0.00013
2,500	0	4.08	3.4
	10	0.0373	0.03
	20	0.0093	0.008
	50	0.0016	0.0013
	100	0.0004	0.00034
5,000	0	4.08	6.83
	10	0.037	0.062
	20	0.0093	0.016
	50	0.0016	0.003
	100	0.0004	0.0007
10,000	0	4.08	13.7
	10	0.037	0.12
	20	0.0093	0.03
	50	0.0016	0.0054
	100	0.0004	0.0013

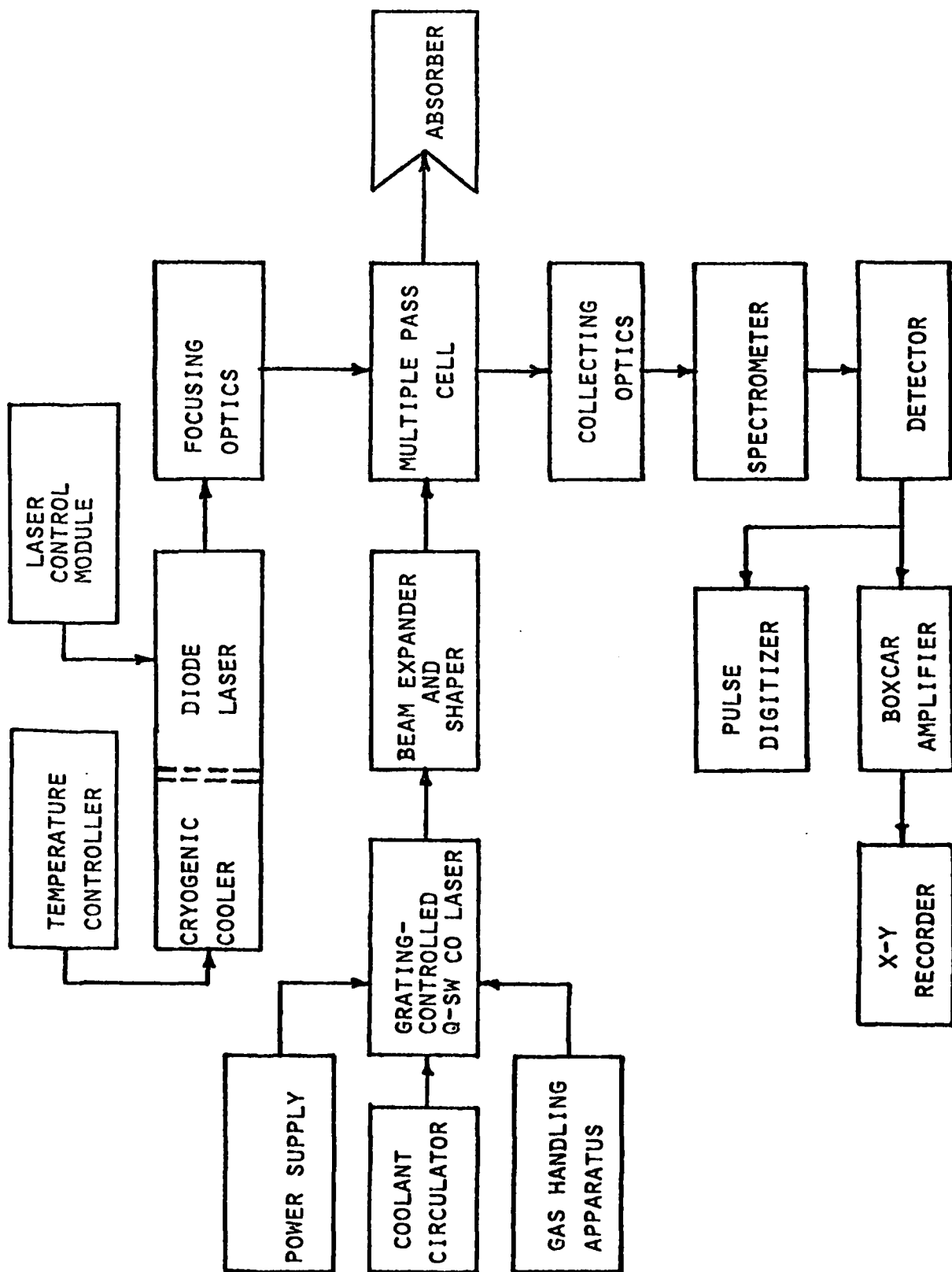


FIG. 1 BLOCK DIAGRAM FOR H₂O LINESHAPE MEASUREMENTS

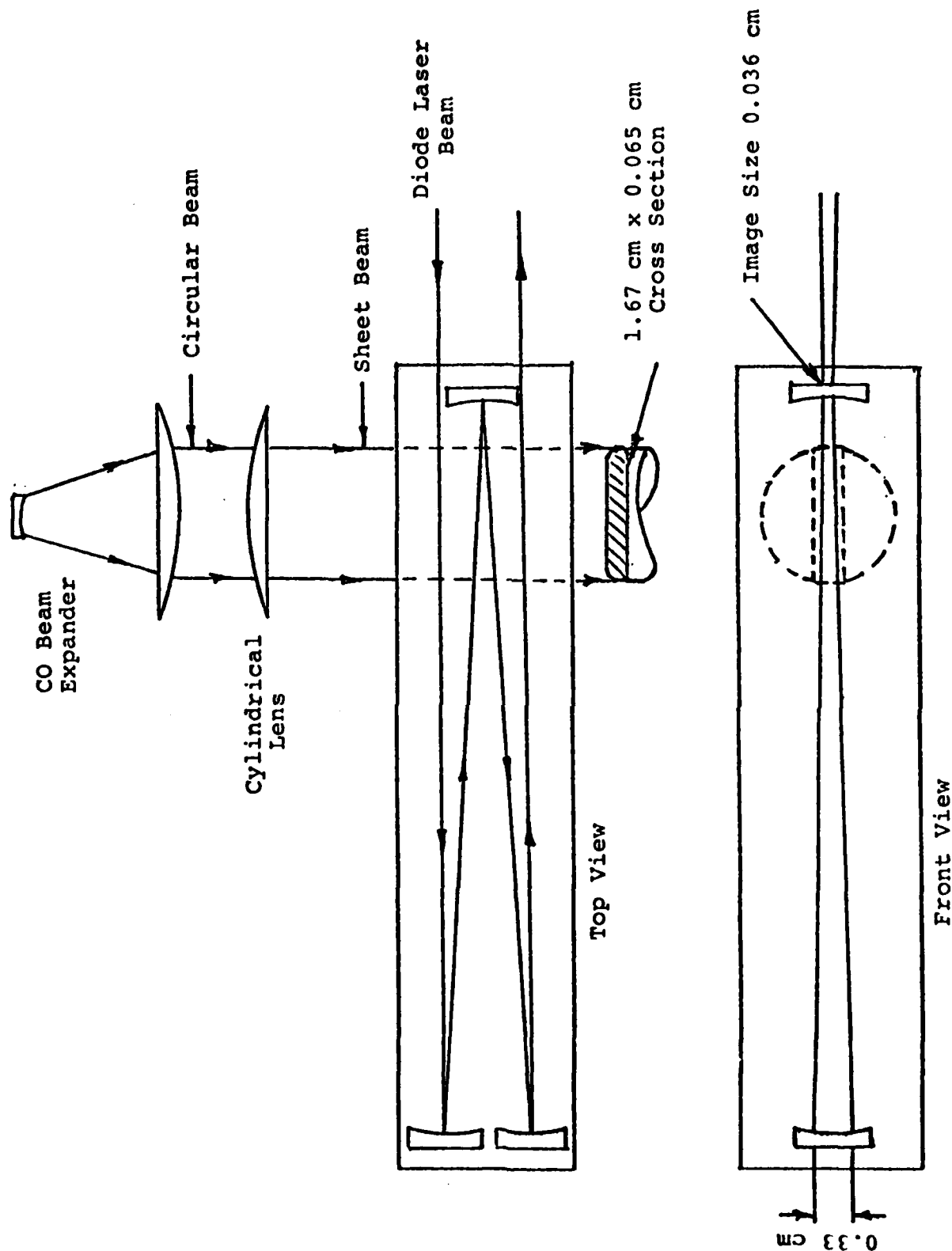


Figure 2
Interaction cell showing CO laser sheet beam overlapping part of diode laser beam.

APPENDIX 1

Calculation of "t" spontaneous (for the 1923.16 cm^{-1} of H_2O).

The line strength is related to the spontaneous transition rate by ²

$$S_{lu} = \frac{c}{8\pi\nu_{lu}^2} \frac{N_l}{P} A_{u \rightarrow l} \frac{g_u}{g_l} \left(1 - e^{-h\nu_{lu}/kT} \right)$$

S_{lu} = line strength in units of $\text{cm}^{-2} \text{ atm}^{-1}$

l = lower state, u = upper state

c = velocity of light in vacuum $\approx 3 \times 10^{10} \text{ cm/sec}$

ν_{lu} = frequency of transition in Hz $= 1923.16 \times c$

N_l = lower level population in molecules cm^{-3}

P = partial pressure of absorber in atm (taken =1 in our calculation)

T = temperature in $^{\circ}\text{K} = 296^{\circ}\text{K}$

g_u, g_l = degeneracies of upper and lower states (g_u/g_l taken ≈ 1 in our case)

and $e^{-h\nu_{lu}/kT} \approx 0$

$A_{u \rightarrow l}$ = spontaneous transition rate

$$N_l = N e^{-E_r/kT} \left(\frac{1}{Q_r Q_v} \right)$$

N = total # of molecules cm^{-3} , at 1 atm $N = 2.478 \times 10^{19}$

E_r = rotational energy in the ground vib. state

Q_r = the rotational partition function

Q_v = vibrational partition function

$Q_v \approx 1$ at 296°K

Q_r is given by ³

$$Q_r \approx \sqrt{\frac{\pi}{ABC} \frac{kT}{hc}}^3 = 1.02718 \sqrt{\frac{T^3}{ABC}}$$

where A, B, C are the rotational constants and for water²,
 $A = 27.8 \text{ cm}^{-1}$, $B = 14.5 \text{ cm}^{-1}$ and $C = 9.28 \text{ cm}^{-1}$

$$Q_r \approx 85 \text{ at } T = 296^\circ\text{K}$$

E_r for an assymetric top is given by ²

$$\frac{E_r(J,K)}{hc} \approx \sqrt{BC} J(J+1) + (A - \sqrt{BC}) K^2$$

J = rotational quantum number.

K = quantum number for the angular momentum component about the figure axis.

The second term is only a small fraction of the first, and hence can be neglected in a first approximation; therefore

$$\frac{E_r(J,K)}{hc} \approx \sqrt{BC} J(J+1)$$

For the 1923.16 cm^{-1} , $E_r(J,K) \approx 648 \text{ cm}^{-1}$.

$$N_l \approx 1.4 \times 10^{16} \text{ molecules cm}^{-3}.$$

The value of S_{lu} (for 1923.16 cm^{-1} line) is ⁴

$$\begin{aligned} S_{lu} &= 1.04 \times 10^{-20} \text{ molecule}^{-1} \text{ cm}^{-2} \\ &= 0.258 \text{ cm}^{-2} \text{ atm}^{-1} \end{aligned}$$

Using these values of S_{lu} , N_l and ν_{lu} , we get

$$\begin{aligned} t_{\text{spontaneous}} &= 17.4 \times 10^{-3} \text{ sec} \\ &= 17.4 \text{ msec.} \end{aligned}$$

APPENDIX 2

The induced transition rate in sec^{-1}

$$\frac{\lambda^2(\nu)}{8\pi n^2 h \nu t_{\text{spontaneous}}} \cdot I(\nu)$$

λ = wavelength of transition in cm

$g(\nu)$ = lineshape function

n = refractive index of the medium ≈ 1

I_ν = laser power density in ergs. cm^{-2}

For the 1923.16 cm^{-1} , therefore,

$$\lambda^2 = 27.04 \times 10^{-8} \text{ cm}$$

$$t_{\text{spontaneous}} = 17.4 \times 10^{-3} \text{ sec.}$$

At line center $g(\nu) = \frac{2}{\pi \Delta \nu}$ (assuming a Lorentzian line shape).

$\Delta \nu(\text{FWHM})^4 = 2 \times (0.078) \text{ cm}^{-1}$ for a mixture of ~ 10 Torr N_2 and ~ 750 Torr H_2O .

h = Planck's const = $66254 \times 10^{-27} \text{ ergsec}$

ν = $1923.16 \times 3 \times 10^{10} \text{ Hz}$

$I(\nu) = 10^7 \times \text{Laser Power in Watts cm}^{-2}$

$W(\nu) = (4.4 \times 10^3) \times (\text{Laser Power in Watts}) \text{ cm}^{-2}$.

REFERENCES

1. Walter J. Moore, "Physical Chemistry," Prentice-Hall, Inc., 3rd ed. 1963, Ch. 7.
2. S. S. Penner, "Quantitative Molecular Spectroscopy and Gas Emissivities," Addison-Wesley, Inc., 1959, Ch. 2, Ch. 7.
3. G. Herzberg, "Infrared and Raman Spectra of Polyatomic Molecules," D. Van Nostrand Co., Inc., 1959, Ch. 5.
4. R. A. McClatchey et al., AFCRL Atmospheric Absorption Line Parameters Compilation, AFCRL-TR-73-0096 (January 1973).
5. C. Freed and H. A. Hans, "Lamb Dip in CO Lasers," IEEE J. Quantum Electron, QE-9 (2), 219 (1973).
6. W. S. Benedict, M. A. Pollack and W. J. Tomlinson III, "The Water-Vapor Laser," IEEE J. Quantum Electron, QE-5 (2), 108 (1969).
7. J. Finzi, F. E. Hovis, V. N. Panfilov, P. Hess and C. B. Moore, "Vibrational Relaxation of Water Vapor," J. Chem. Phys., 67 (9), 4053 (1977).

END

DATE
FILMED

10-8

DTIC



AD-A089 071 LASER ANALYTICS INC BEDFORD MA

F/B 7/4

HIGH RESOLUTION TUNABLE DIODE LASER MEASUREMENTS OF WATER..ETC.(U)

MAR 78 ENG.R.S.; MANTZ, A.W.

F19628-77-C-0015

UNCLASSIFIED

AFGL TR-79-0239 PROJ. 2310 TASK G1

N/L

2 x 2

CLASSIFICATION

INFORMATION

END

DATE

VIEWED

7-81

DTIC

DA
089

SUPPLEMENTAR

INFORMATION

AD-A089071

absorption from LOWTRAN 3B. (24) The dashed straight line was obtained by linear least squares fitting, the slope of which is about 9.5% greater than that of the calculated value using LOWTRAN 3B data. The data from Montgomery (22) taken at 1250 cm^{-1} also showed a higher value for the continuum absorption coefficient at the same temperature (he actually used nitrogen at one atmosphere for broadening; since the contribution from nitrogen broadening is negligible, he essentially measured the self continuum absorption coefficient). All of the observed data reported here were for pure water vapor as attempts to observe the contribution from nitrogen broadening at 760 torr N_2 was not successful because the contribution was too small to be measurable for the pathlength and pressures used.

AFG-1-76-79-12-1

The pressure squared dependence was also observed at room temperature at 296K. Figure 4 is a plot of the continuum absorbance vs. pressure squared at 295.8K. The solid curve again represents calculated values using a LOWTRAN 3B formula. The observed values are slightly smaller than the calculated values. Our observed values are somewhat closer to those reported by Shumate et. al. (10) who used a CO_2 laser and a spectrophone for their measurements. Note that although the absorbance is smaller, the uncertainty of the absorbance is proportionally smaller because the absorption cell temperature was much more uniform and stable at room temperature.

Because of the very high resolution and tunability of diode laser, we were able to observe both local line and continuum absorptions by tuning the laser through moderately strong absorption lines. Figure 5 is a plot of the absorbance αL vs. wavenumber near the water vapor line at 1014.45 cm^{-1} with transition designated by $10_{1,10} + 11_{2,9}$. This line was accurately measured previously. (17) The solid line is the experimental curve and the dotted line is the theoretical curve obtained by nonlinear least squares fitting a Lorentzian line and a flat continuum absorption. While there are 512 digitized points for the frequency axis,

about 35 of these near the line center were not used in the fit because of their large uncertainty. Three parameters were obtained in the fit program, namely, the line strength, halfwidth and the continuum absorption coefficient. The pathlength was 80.1m; the vapor pressure was 58.9 ± 0.6 torr, and the cell temperature was 337 ± 2 K. The transmission peaks of a 1 inch Ge etalon were used to obtain a relative frequency scale. The observed intensity, halfwidth and continuum absorbance (αL) are $3.83 \times 10^{-23} \text{ cm}^{-1} \text{ mol}^{-1} \text{ cm}^2$, 0.021 cm^{-1} and 0.118 respectively. The first two values are in good agreement with previous data.⁽¹⁷⁾ The continuum absorbance appears to be more than 20% higher than the calculated value based on LOWTRAN 3B.

We have measured the continuum absorption at a number of frequency in the $950\text{--}1050 \text{ cm}^{-1}$. Figure 6 is a plot of the self continuum absorption coefficient C° vs. frequency at temperature of 296 ± 0.5 K. The circles are experimental points. The solid curve is calculated using a LOWTRAN 3B formula. The agreement is fair over most of the spectral region. At higher temperatures we have also measured the self continuum absorption coefficient C° . Figure 7 is a plot of C° vs. frequency for two temperatures, 333K and 337K. At each temperature, the observed values of C° is slightly greater than the calculated values indicating a slightly weaker temperature dependence for C° than that in LOWTRAN 3B. Based on our experimental data, the temperature dependence parameter T_0 at 1002.0 cm^{-1} is about 1540K, which is significantly below the suggested value of 1800K.⁽²³⁾ Although the value 1540K is not entirely unexpected,⁽²⁾ it is slightly out of the typical range. Whatever the implication this has with regard to the source of continuum absorption, it is worth further investigating.

As mentioned in the preceding paragraph, the observed continuum absorption at 337K near a moderately strong line has been found to be significantly greater than the value based on LOWTRAN 3B. Furthermore, we have also observed that near the line